



Effects of the infill pattern on mechanical properties of fused layer modeling (FLM) 3D printed wood/polylactic acid (PLA) composites

S. Kain¹ · J. V. Ecker² · A. Haider² · M. Musso³ · A. Petutschnigg¹

Received: 13 February 2019 / Published online: 25 November 2019
© Springer-Verlag GmbH Germany, part of Springer Nature 2019

Abstract

In this paper, possible influences of various infill orientations (deposition angles) on specific material characteristics—such as tensile strength, compressive strength, charpy impact strength and heat deflection temperature (HDT)—of fused layer modeling (FLM) processed test specimens were evaluated. Two specially made wood filaments, made of the same polylactic acid (PLA) polymer but two different wood fiber contents, were used for sample manufacturing and evaluated as a function of fiber content as well as infill orientation. In the context of the wood fiber content, formulations containing 15 wt. % as well as 25 wt. % of fibers were examined. In connection with infill orientation, the influence factor of seven FLM 3D printing infill orientations (deposition angles)—in particular 0°, 15° crossed, 30° crossed, 45° crossed, 60° crossed, 75° crossed and 90°—on several material properties was investigated. It could be proven that there is a direct interaction between the infill orientation (deposition angle) and the resulting mechanical performance of the test specimens. This is not exclusively a direct correlation, but there is a mutual dependency. Apart from that, the analysis showed that the higher the fiber content in the filament, the higher the resulting mechanical properties.

1 Introduction

Additive manufacturing (AM), also referred to as layer manufacturing (LM), is a widely used collective term describing a group of various process technologies applied to produce physical three-dimensional objects from virtual computer aided design (CAD) models (Hague et al. 2001; Mansour and Hague 2003; Chua et al. 2014). Compared to the common manufacturing process, AM has some interesting advantages, including the possibility to produce complex-shaped objects without using casting molds or special tools (Wimmer et al. 2015; Ecker et al. 2017). For this reason AM

is very well suited for customizing products or for producing functional prototypes (Wimmer et al. 2015).

FLM, part of the AM family, operates with a wide range of suitable prefabricated thermoplastic polymers in the shape of a continuous wire, referred to as filament (Gebhardt 2012; Ecker et al. 2017). FLM describes the layer-by-layer deposition of thermoplastic material, which is continuously transported to the print head to be melted and afterwards deposited by means of a nozzle for building up a three-dimensional object (Gebhardt 2012). In AM processes, the materials are utilized very efficiently, resulting in very little or zero waste (Berman 2012), which has become increasingly essential in recent years (Kariz et al. 2018).

In the 21st century, due to concerns regarding the sustainability as well as the environment, there has been a rethinking in the field of natural fiber-reinforced composites (NFCs), made from non-petroleum based polymers. Companies all around the world are attempting to increase the usage of these natural fiber-reinforced biopolymers (Mohanty et al. 2002; Faruk et al. 2012). Apart from expected ecological advantages, like CO₂ balance, sustainability, recyclability, biological degradability (Wollerdorfer and Bader 1998; Joshi et al. 2004; Mohanty et al. 2005; Holbery and Houston 2006) as well as cost saving issues of natural fibrous materials, these reinforcing fillers provide some attractive intrinsic

✉ S. Kain
stefan.kain@fh-salzburg.ac.at

✉ J. V. Ecker
sirjiv@gmail.com

¹ Department of Forest Products Technology and Timber Construction, Salzburg University of Applied Sciences, Kuchl, Austria

² Department of Bio-based Composites and Processes, Kompetenzzentrum Holz GmbH (Wood K Plus), Linz, Austria

³ Department of Chemistry and Physics of Materials, University of Salzburg, Salzburg, Austria

properties concerning density and mechanical behavior (Kalia et al. 2011). NFCs have an anisotropic nature in terms of mechanical properties, due to the fiber orientation along the flow direction while processing them. Thus, the mechanical performance of NFCs is based on the extent of oriented fibers. The efficiency of transferring loads is much better when both, the orientation of fiber reinforcement and the load direction are identical (Geethamma et al. 1998).

Numerous groups of researchers have already reported on the usage of wood fibers as reinforcement material in many various thermoplastic polymers, mainly because of low prices—they are less expensive than synthetic fibrous materials—and sufficient availability (English and Falk 1995; Oswald 1999; Williams and Wool 2000; Bledzki and Faruk 2003; Stark and Rowlands 2003; Peltola et al. 2014). Additionally, natural fibrous fillers provide low densities (Holbery and Houston 2006), which in turn lead to lighter weight structures when compared to inorganic fillers like glass fibers (Summerscales et al. 2010) or carbon fibers.

In recent studies, different FLM 3D printable fiber-reinforced composites were tested and analyzed: Gkartzou et al. (2017) investigated the effect of fused filament fabrication (FFF) 3D printed test specimens using bio-based blends of PLA and low-cost kraft lignin—with various weight ratios—on specific thermal, morphological and mechanical characteristics. Furthermore, they analyzed several process parameters, which have an impact on shear rate as well as stress imposed on the melt (Gkartzou et al. 2017).

Murphy and Collins (2018) developed novel, fully biodegradable and fused deposition modeling (FDM) 3D printable microcrystalline cellulose (MCC) reinforced PLA filaments, having final concentrations of 1, 3 and 5 wt. % of cellulose. The influence of the cellulose content in the filament on the thermal, morphological and mechanical characteristics was investigated. A dynamic mechanical thermal analysis illustrated an increase in storage modulus concerning all MCC reinforced PLA filaments. The analysis by means of differential scanning calorimetry (DSC) proved that crystallinity of all biocomposites increased (Murphy and Collins 2018).

Le Duigou et al. (2016) reported that the mechanical performance of FDM 3D printed biocomposites using wood filament depends very much on the printing orientation. In this study, a printing orientation of 0° and 90° was applied to investigate the influence of the printing orientation on mechanical properties, such as tensile strength. Furthermore, the mechanical performance as a function of the printing width (overlapping of filaments) was also evaluated. Besides, Le Duigou et al. (2016) examined the water uptake as well as swelling behavior of test specimens made by means of FDM as a function of the time. The results showed that an increased printing width lowers the cohesion of the FDM 3D printed biocomposites, but

improves the porosity, which in turn leads to a decrease in tensile strength and to a massive increased water absorption (Le Duigou et al. 2016).

Tao et al. (2017) produced a wood filament using a PLA polymer and added a wood particle content of 5 wt. %. An investigation of the tensile strain–stress behavior of the 3D printed test specimens was carried out. Additionally, SEM images of the fractural surfaces were taken in order to analyze the morphological structure (Tao et al. 2017).

Pandey (2015) compounded various natural fibers with different thermoplastic polymers (polypropylene, polyethylene as well as polystyrene) and analyzed the compounds for their suitability. In addition, a wood filament UPM ForMi (cellulose fiber-reinforced plastic composite), consisting of 40 vol. % cellulose fibers, was also tested for its suitability (Pandey 2015).

Kariz et al. (2018) investigated the effect of different wood contents (0–50%) in FDM filaments on tensile strength, tensile modulus and rheological properties. They found out that the tensile strength of the wood filaments increased by 55–57 MPa for NFCs containing 10% of wood fibers, but decreased steadily with higher filler contents to 30 MPa for wood filaments containing 50% of wood fibers (Kariz et al. 2018).

Based on these considerations, the following research question should be answered in this study:

Whether and to what extent the infill orientation (deposition angle) of FLM 3D printed wood fiber-reinforced composites is influencing specific mechanical properties, like tensile strength, compressive strength, impact strength as well as HDT.

2 Materials and methods

2.1 Wood filaments

All wood filaments used for sample manufacturing were produced using the manufacturing facilities from Wood K Plus situated in Linz (Austria). Various recipes were applied to fabricate these wood filaments, using pre-dried PLA granulate (Ingeo™ 3251D) provided by NatureWorks, Minnetonka, USA, which was utilized as thermoplastic for the polymer matrix. This sort of PLA has a glass transition temperature of 55–60 °C, specific gravity of 1.24 g * cm⁻³ and MFR (melt mass-flow rate) of 80 g * 10 min⁻¹ (210 °C, 2.16 kg). For all wood filaments, one and the same PLA polymer was used in which wood fibers (ARBOCEL® C100; provided by JRS J. Rettenmaier & Söhne, Rosenberg, Germany) were embedded. The grain size of the wood fibers ranged between 30 and 200 µm.

Table 1 Comparison of the different wood filaments used

Identification	Components/ingredients	
	PLA (Ingeo™ 3251D)	Wood fibers (ARBOCEL® C100)
#1 (85/15)	85 wt. %	15 wt. %
#2 (75/25)	75 wt. %	25 wt. %

2.2 Preparation of NFCs

The PLA granulate (Ingeo™ 3251D) as well as the wood fibers (ARBOCEL® C100) were pre-dried in the dry kiln DRYMAX E30 Aton 2 (WITTMANN BATTENFELD, Kottingbrunn, Austria) at a temperature of 60 °C for about 12 h. Two different formulations were applied to the NFC filament production without adding any kind of additives to the compounds. Table 1 shows the exact composition of the custom-made wood filaments used for sample manufacturing.

The mixed components were then merged using a lab scale co-rotating compounder (TSE) from Brabender, Duisburg, Germany. The twin-screws of this compounder have a diameter of 20 mm and a length/diameter (L/D) ratio of 40. The following temperature extruder-profile was set during production: the feeding zone was maintained at 170 °C, 170 °C for the compression zone, and the metering zone was maintained at 170 °C. Furthermore, a screw speed of 350 rpm and a torque ranging from 20 up to 40 Nm was required for manufacturing the wood filaments. For granulate pelletizing an underwater pelletizing line (EUP 50) from ECON, Weisskirchen, Austria, was utilized. Prior to further processing steps, the NFC compound granulate was again dried in the same dry kiln using similar drying conditions (60 °C for about 12 h).

The final compounding process was done utilizing the same counter-rotating conical twin-screw extruder, but applying a modified temperature profile: the feeding zone was set to 170 °C, 170 °C for the compression zone, while the metering zone was maintained at 190 °C. Furthermore, the screw speed was set to 110 rpm and the torque ranged from 20 up to 40 Nm. The extruder was equipped with a belt conveyor for calibration, a haul-off unit for controlling the speed, and a winder for winding up the solid plastic wire on a spool. The diameter of the wood filaments was maintained at 1.75 mm. An online two-laser measurement system (Accuscan 5012 from Beta LaserMike, High Wycombe, United Kingdom) was used for monitoring and controlling the diameter accuracy of the endless solid plastic wire. For minimizing the variation in filament diameter, many different process parameters, like processing temperature, humidity of the compound, diameter of the extruder nozzle,

crystallinity of the used PLA as well as take-off speed, were systematically optimized and adjusted.

2.3 Sample manufacturing

An Ultimaker 2+ (Ultimaker, Geldermalsen, the Netherlands) was utilized for test specimen production. To avoid any formulation influences arising from deviations in the filament composition, the studies were conducted with two specially made wood filaments, using the same PLA polymer (Ingeo™ 3251D) with two different wood fiber contents (ARBOCEL® C100). One filament contained a fiber content of 15 wt. % while the other was made using 25 wt. % of wood fibers. Furthermore, both custom-made wood filaments had a diameter of 1.75 mm.

For slicing all virtually constructed test specimens and for defining the process parameters for the FLM 3D printer, the company's own slicing software Cura (version 3.2.1) was applied. All printing parameters (see Table 2) performed best in several preliminary trials and were therefore applied as default settings for manufacturing all FLM 3D printed samples.

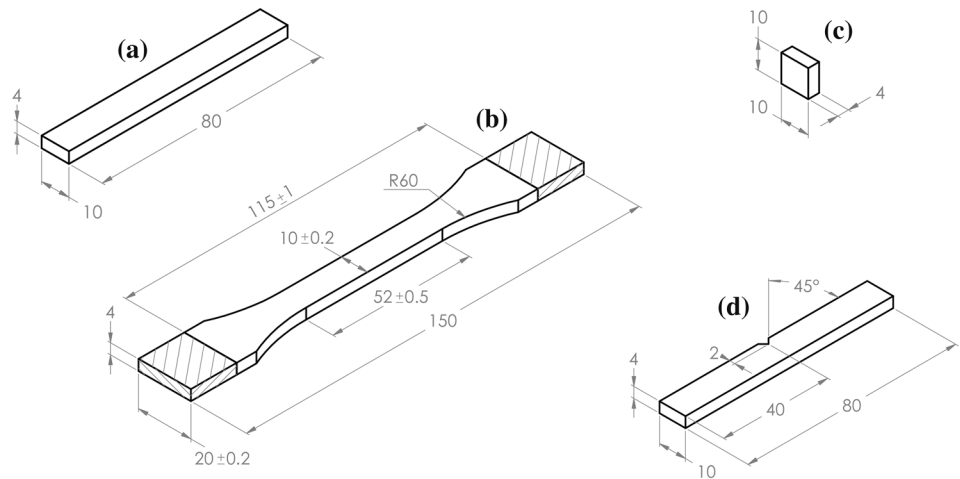
2.4 Specimen geometry

Figure 1 shows the various geometries that were applied to produce all the samples by means of the FLM 3D printer Ultimaker 2+. The tensile test specimens were manufactured in “dog-bone” shape according to ÖNORM EN ISO 527-4 (1997). All dimensions were taken into account as specified in the above-mentioned standard (geometry type 1B) with a thickness of 4 mm and a gauge length of 52 mm. The charpy impact strength samples (unnotched) as well as the HDT specimens were constructed as a three-dimensional

Table 2 All the specific print settings for producing the test specimens FLM 3D printer: Ultimaker 2+ from Ultimaker

Nozzle diameter	0.6 mm
Layer height	0.2 mm
Wall thickness	1 Perimeter (0.6 mm)
Infill/infill density	99.9% (rectilinear)
Initial layer speed	10 mm * sec ⁻¹
Initial wall speed	10 mm * sec ⁻¹
Initial infill speed	10 mm * sec ⁻¹
Print speed	22.5 mm * sec ⁻¹
Wall speed	13.5 mm * sec ⁻¹
Infill speed	13.5 mm * sec ⁻¹
Printing temperature	210 °C
Build plate temperature	60 °C
Build plate adhesion	UHU Stick (UHU® UHU Klebestift “Stic” 40 g)

Fig. 1 Various geometries for testing specific mechanical properties of the FLM 3D printed test specimens, made from two specially made wood filaments. **a** Charpy impact strength (unnotched) and HDT, **b** tensile strength, **c** compressive strength, and **d** charpy impact strength (notched). Dimensions in [mm]

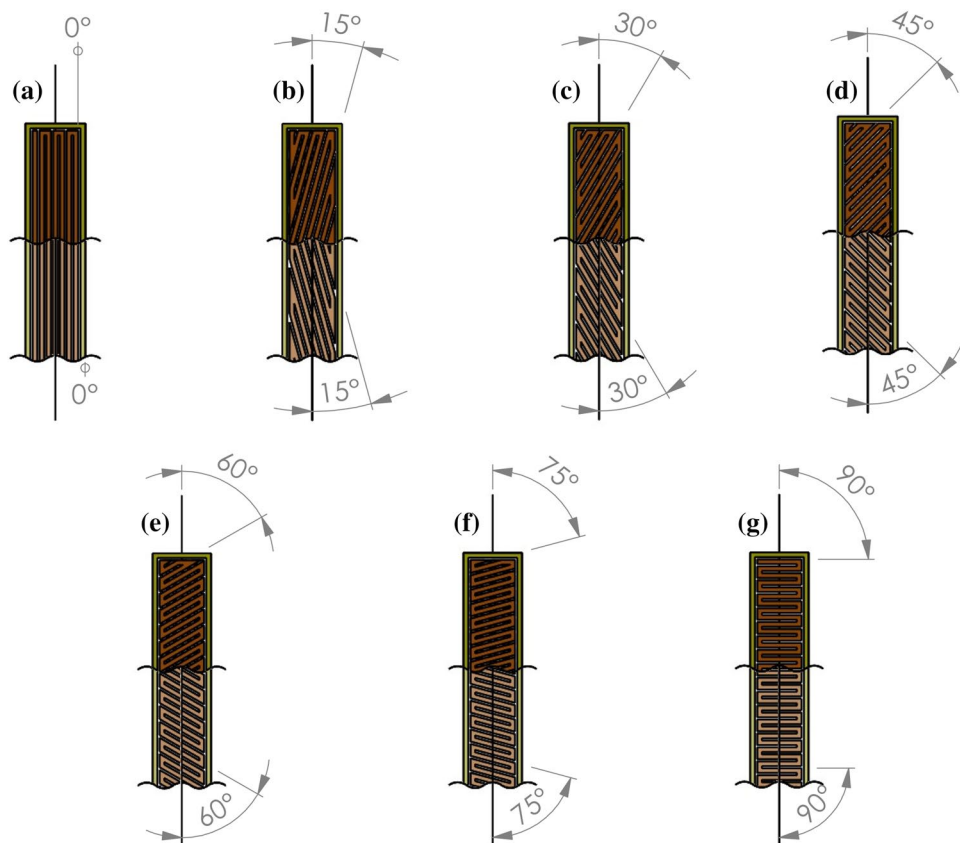


CAD geometric model (Fig. 1), having a length of 80 mm, a width of 10 mm, and a thickness of 4 mm. Once the unnotched Charpy samples were FLM 3D printed, a 45° V-shaped notch having a depth of 2 mm was centrally cut into half of the unnotched Charpy specimens to get notched ones. The design of the samples for investigating the compressive strength was geometrically compliant to ÖNORM EN ISO 604 (2003) having a length and a width of 10 mm as well as a thickness of 4 mm.

2.5 Infill orientations

The infill orientations (deposition angles) imaged in Fig. 2 were applied to produce all the FLM 3D printed wood fiber-reinforced composites.

Fig. 2 All seven infill orientations applied for manufacturing the test specimens. **a** 0°, **b** 15° crossed, **c** 30° crossed, **d** 45° crossed, **e** 60° crossed, **f** 75° crossed and **g** 90°



2.6 Testing

The measured data of the FLM 3D printed wood fiber-reinforced biocomposites were processed and analyzed using Microsoft Excel (version 15.33).

2.6.1 Tensile strength

All investigations were conducted at a controlled temperature of 23 °C while the relative humidity was maintained at a constant level of 50%, according to the above-mentioned standard ÖNORM EN ISO 527-4 (1997). All in all, 70 samples made from two specially made wood filaments—the same PLA polymer with two different wood fiber contents (15 wt. % and 25 wt. %)—with seven various infill orientations (deposition angles) were tested. Depending on the infill orientation applied and per fiber content, a total of five identical “dog-bone” shaped samples were examined.

A universal material testing machine (Zwick/Roell Z250 from Zwick Roell Group, Ulm, Germany) equipped with an add-on device for testing the tensile strength and a 20 kN load cell (Zwick/Roell type: Xforce K) was utilized. The cross-head speed was maintained at 10 mm * min⁻¹ and the initial distance between the lower and upper grip was set to 115 mm. The resulting clamping length was 17.5 mm. During testing, the ultimate tensile strength and the travelled distance were both determined for each sample.

2.6.2 Compressive strength

The same universal material testing machine that was utilized for examining tensile strength was also used for testing the compressive strength of the FLM 3D printed samples. In this case, the testing machine was equipped with an add-on device for testing the compressive strength and a 250 kN load cell. The cross-head speed during compressive testing was also maintained at 10 mm * min⁻¹. During testing, the compressive strength and the travelled distance were both determined for each test specimen. All measurements were conducted according to the standard ÖNORM EN ISO 604 (2003). Depending on the infill orientation applied and per fiber content, a total of five identical compressive specimens were investigated.

2.6.3 SEM analysis

In order to gain an impression of the possible morphological structure differences of the FLM 3D printed wood fiber-reinforced composites, a SEM analysis was conducted on fractural surface areas. SEM micrographs of the “dog bone” fracture surfaces were obtained on a Phenom ProX Desktop SEM microscope (Thermo Fisher Scientific, Waltham, USA), which was equipped with a field emission gun. The

fractural areas of the tensile specimens were analyzed perpendicular to the fractured surface, without applying any coating—that would prevent static electricity—using an electrical voltage of 15 kV and a magnification of 300–500 times.

2.6.4 Charpy impact strength (unnotched and notched specimens)

Charpy impact testing of the FLM 3D printed wood fiber-reinforced composites was conducted by an instrumented pendulum impact tester CEAST 9050 (Instron, Darmstadt, Germany). Both, system control as well as data analysis were performed according to DIN EN ISO 179-1 (2010). The testing apparatus was equipped with a hammer that has an impact energy of 0.5 J. The impact measurements were taken under controlled conditions having a temperature of 23 °C and a relative humidity of 50%. Depending on the infill orientation applied and per fiber content, a total of ten identical impact bar specimens were investigated.

2.6.5 HDT (Heat deflection temperature)

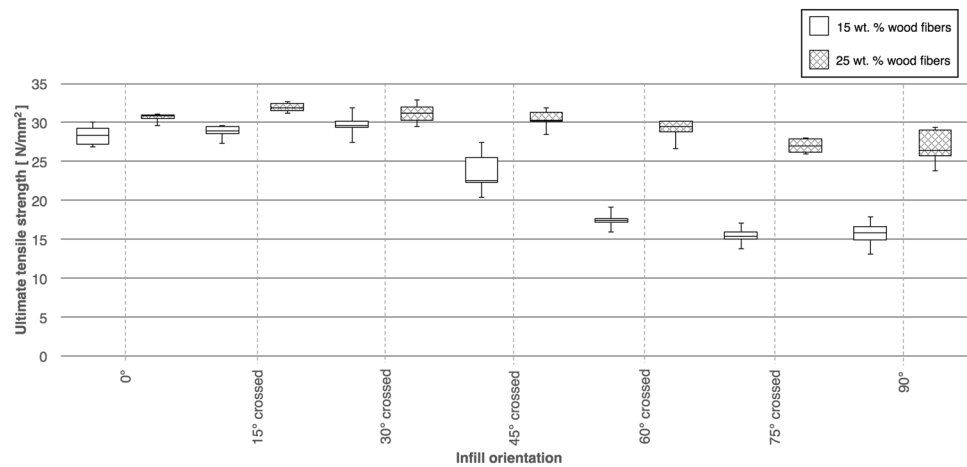
All measurements were performed on a CEAST HDT 3 (Instron, Darmstadt, Germany) using the following temperature profile for testing: temperature rise in steps of 2 °C * min⁻¹. HDT of the FLM 3D printed wood fiber-reinforced composites was analyzed according to the standard DIN EN ISO 75-1 (2013a) as well as DIN EN ISO 75-2 (2013b). Variation HDT/B was applied—in which the bending load is set to 0.45 MPa—for all investigations. As soon as the deformation exceeds 0.2%, its temperature could be measured. Depending on the infill orientation applied and per fiber content, a total of three identical HDT samples were examined.

3 Results and discussion

3.1 Tensile strength

An analysis of the tensile strength, which can be seen in Fig. 3, indicates that the highest measured tensile strength is not as expected at 0° infill orientation. However, the maximum tensile strength could be achieved between 15° crossed and 30° crossed, depending on the fiber content of the wood filament used. Generally, Fig. 3 demonstrates that the infill orientation has an influence on the ultimate tensile strength behavior. However, the effect of the infill orientation is more pronounced for the wood fiber-reinforced composites having a fiber content of 15 wt. %. In this case, a change in infill orientation from 0° (print direction and load direction are similar) to 90° (print direction and load direction are

Fig. 3 Box plot chart showing the ultimate tensile strength behavior depending on the infill orientation applied as well as the fiber content used in the wood fiber-reinforced composites



perpendicular to each other) leads to a decrease in tensile strength of about 50% from 28 to 16 N/mm².

The behavior of the ultimate tensile strength is assumed to be related to the interaction of the deposition angle (infill orientation) of the print head. As described in the literature, incorporation of fibers into the polymer structure creates NFCs, which are characterized by high mechanical properties, including tensile modulus as well as flexural modulus (Stark and Rowlands 2003; Peltola et al. 2014; Wang et al. 2017).

3.2 Compressive strength

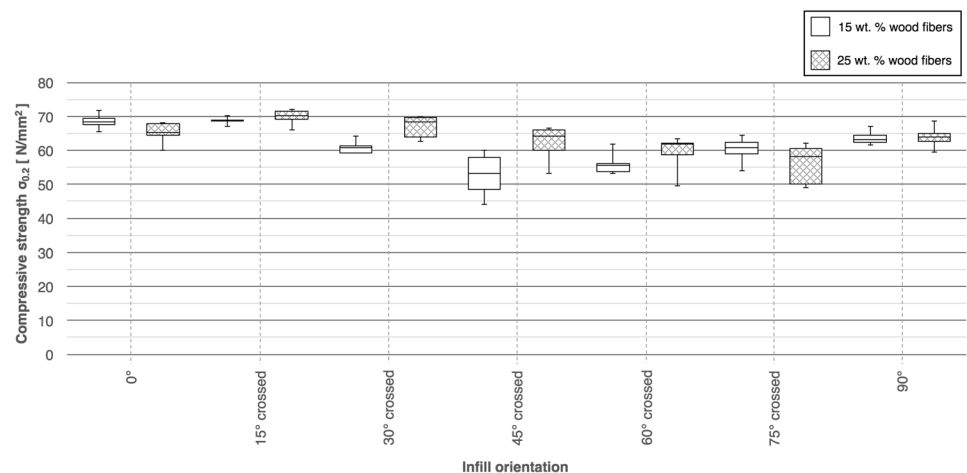
Figure 4 shows the measured compressive strength of the test specimens as a function of the infill orientation as well as the fiber content of the wood fiber-reinforced composites. The compressive strength behavior is similar to the diagram representing the tensile strength of the FLM 3D printed wood fiber-reinforced composites having a fiber content of 15 wt. %, but not so pronounced. As expected, the highest possible compressive strength could be measured when the

infill orientation is set to 0° as well as 15° crossed. In this case, the infill orientation (deposition angle) is equal to the applied compressive force, which guarantees the best possible load transfer. In terms of compressive strength, it can be claimed that FLM 3D printed wood fiber-reinforced composites having a fiber content of 25 wt. % tend to have a higher compressive strength, regardless of the infill orientation, in comparison to the samples with 15 wt. % of wood fibers.

3.3 SEM analysis

Figures 5 and 6, both indicate the connection quality of adjacent filament strands of FLM 3D printed wood fiber-reinforced composites. It can be seen that the connection quality of adjacent filament strands is much better when an infill orientation like 15° crossed or 30° crossed is used for producing the test specimens (see Fig. 5). When comparing the SEM picture showing a 15° crossed infill orientation to the SEM picture showing a 90° infill orientation (see Fig. 6), a significantly poorer connection quality of adjacent filament strands is recognizable at first glance.

Fig. 4 Box plot chart showing the compressive strength $\sigma_{0.2}$ behavior depending on the infill orientation applied as well as the fiber content used



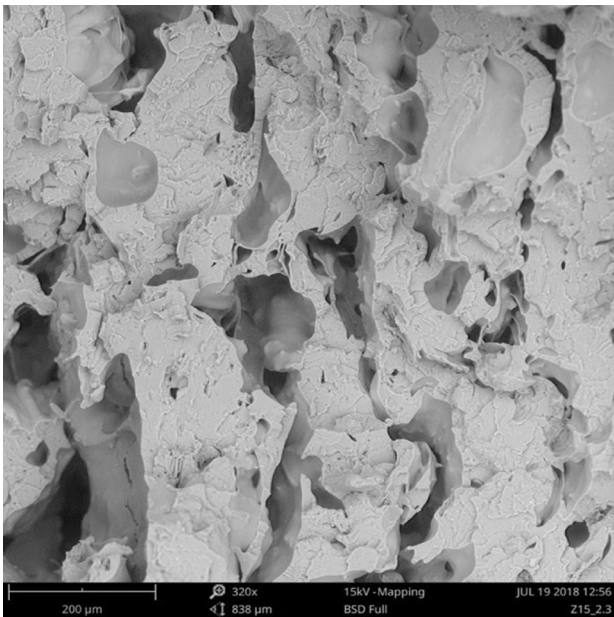


Fig. 5 This SEM picture shows the fracture surface of a FLM 3D printed tensile specimen having an infill orientation of 15° crossed using a wood filament with a fiber content of 15 wt. %



Fig. 6 This SEM picture illustrates a fracture surface of a FLM 3D printed tensile specimen having an infill orientation of 90° using a wood filament with a fiber content of 15 wt. %. It can be seen that adjacent filament strands are only connected in a few spots (marked in black) with each other

The voids (defects) highlighted in black on the SEM picture (see Fig. 7) are caused by the moisture contained in the filler material; wood fibers have a hydrophilic nature

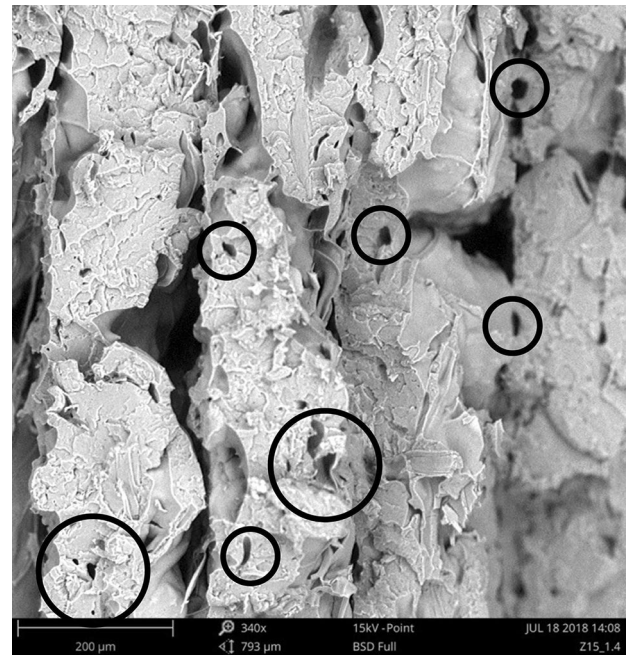


Fig. 7 SEM picture showing the fracture surface of a tensile specimen, which was FLM 3D printed with an infill orientation of 0° using the wood filament with a fiber content of 15 wt. %. The black colored spots are voids, which negatively affect the mechanical properties of the wood fiber-reinforced composites

(Takatani et al. 2008), which changes to vapor state during extrusion and thus forms these defects in the FLM 3D printed sample.

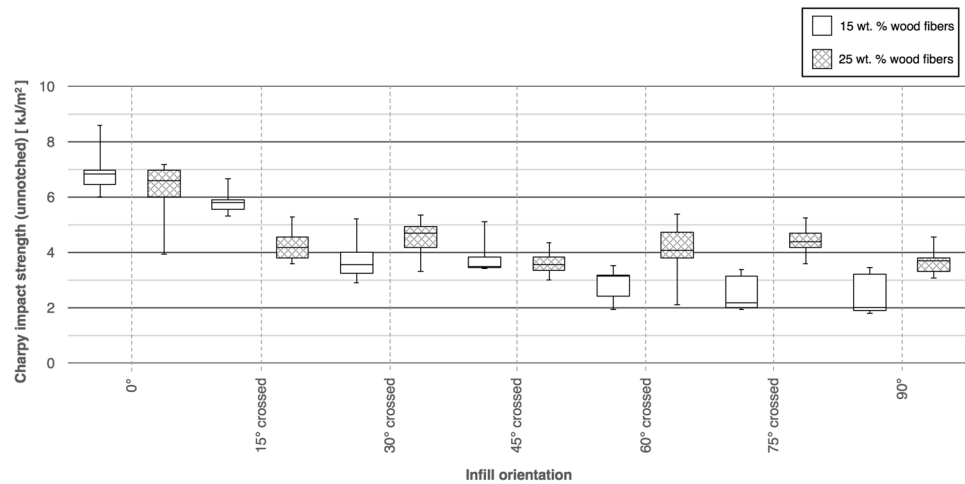
3.4 Charpy impact strength (unnotched)

The charpy impact strength evaluation shows that FLM 3D printed samples having an infill orientation of 0° had the highest possible values of all tested specimens (see Fig. 8). The more the infill orientation (deposition angle) shifts towards 90° , the more the resulting impact strength decreases noticeably. A very similar behavior, a decrease in mechanical performance with increasing infill orientation, could be recognized for the tensile strength.

Basically, Fig. 8 demonstrates that the infill orientation has a noticeable influence on the charpy impact strength, especially for the FLM 3D printed samples having a fiber content of 15 wt. %. A steady decrease in the measured material characteristics can be observed, when the infill orientation (deposition angle) shifts from 0° towards 90° . The charpy impact strength starts at an average value of about 6.8 kJ/m^2 (infill orientation is perpendicular to the loading direction) and ends at an average value of 2 kJ/m^2 , a reduction of about 70% in impact strength occurred.

At an infill orientation of 0° as well as 15° crossed, the samples with 15 wt. % fiber content performed better

Fig. 8 Box plot chart showing the Charpy impact strength behavior (unnotched samples) depending on the infill orientation (deposition angle) as well as the wood fiber content

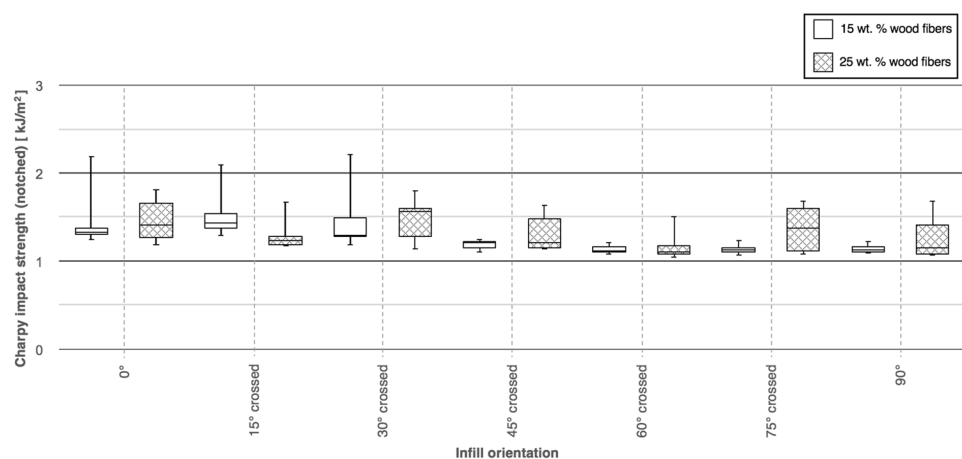


than the test specimens with 25 wt. % wood fibers, but for all other infill orientations (30° crossed, 45° crossed, 60° crossed, 75° crossed and 90°) the samples having a fiber content of 25 wt. % provided equal or much higher impact strength values than the test samples with a wood fiber content of 15 wt. %.

3.5 Charpy impact strength (notched)

For notched specimens, no significant influence of the infill orientation (deposition angle) on the measured Charpy impact strength could be determined, which can be seen in Fig. 9. Only a slightly higher impact strength for the test specimens having a wood fiber content of 25 wt. %, compared to test samples with a fiber content of 15 wt. %, could be observed (except for 15° crossed). All in all, it can be claimed that a higher fiber content has a positive influence on the Charpy impact strength; wood fibers have a positive reinforcing effect on the impact strength.

Fig. 9 Box plot chart showing the Charpy impact strength behavior (notched samples) depending on the infill orientation as well as the fiber content



3.6 Heat deflection temperature (HDT)

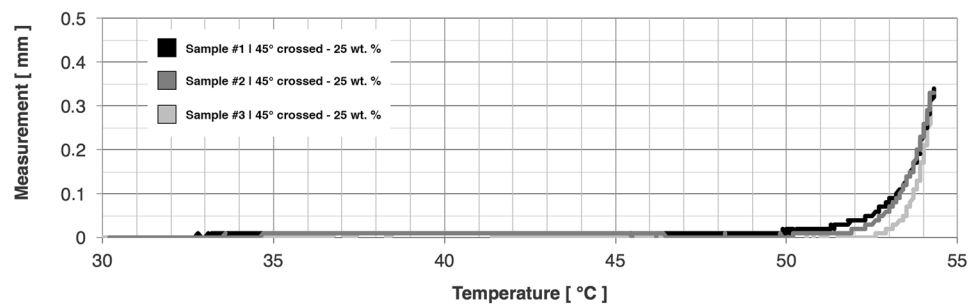
This material characteristic is purely material-dependent and unaffected by the infill orientation. All samples examined showed exactly the same thermal behavior. In addition, the wood filler amount has hardly any effect, since the thermal stability of the NFC is largely dependent on the thermoplastic polymer. Thus, little influence can be detected, whereby the level of significance is not pronounced (see Fig. 10).

4 Conclusion

In the framework of this research, it could be proven that there is a direct interaction between the infill orientation (deposition angle) and the resulting mechanical performance of the test specimens. This is not exclusively a direct correlation, as illustrated in the charts shown in Figs. 3, 4 and 8.

With regard to the wood fiber content used in the two specially made wood filaments (one with 15 wt. % and the other one with 25 wt. % of wood fibers), it could also be demonstrated that a higher proportion of fibers led to noticeably

Fig. 10 Chart showing the thermal behavior of three HDT specimens, which were FLM 3D printed with an infill orientation of 45° crossed using the wood filament with a fiber content of 25 wt. %. All samples examined showed exactly the same thermal behavior



better mechanical properties. At least up to a fiber content of 25 wt. %, an improvement in mechanical properties could be observed. Currently, it is still unclear whether a further increase in fiber content will also result in an improvement of the mechanical characteristics, or whether it will lead to a decrease in mechanical properties. Taking these results into consideration, it is recommended to select the infill orientation (deposition angle) carefully for structural components, exposed to mechanical stress, in order to achieve the best possible mechanical performances of the structural component.

An important step in successfully estimating specific mechanical properties of FLM 3D printed objects is a quantification as well as an investigation of the microstructure of a single fiber, and of the fiber network that is embedded in the thermoplastic polymer matrix (Lux et al. 2011). For future scientific studies dealing with this topic, it is essential to utilize investigative tools which can adequately describe the three-dimensional structure of the fibrous reinforcement material.

Acknowledgements All investigations are implemented within the project Interreg Austria–Bavaria AB 97 TFP HyMat. The major aim of this cooperation is the establishment of hybrid materials, utilizing for example wood filaments for FLM 3D printing. The authors gratefully acknowledge the financial support provided by the European Regional Development Fund and Interreg V-A Program Austria–Bavaria 2014–2020 through the Interreg Austria–Bavaria project AB 97 TFP HyMat.

Compliance with ethical standards

Conflict of interest On behalf of all authors, the corresponding authors state that there is no conflict of interest.

References

- Berman B (2012) 3-D printing: the new industrial revolution. *Bus Horiz* 55(2):155–162. <https://doi.org/10.1016/j.bushor.2011.11.003>
- Bledzki AK, Faruk O (2003) Wood fibre reinforced polypropylene composites: effect of fibre geometry and coupling agent on physico-mechanical properties. *Appl Compos Mater* 10(6):365–379. <https://doi.org/10.1023/A:1025741100628>
- Chua CK, Leong KF, An J (2014) Introduction to rapid prototyping of biomaterials. In: Narayan R (ed) *Rapid prototyping of biomaterials: principles and applications*, 1st edn. Woodhead Publishing, Philadelphia, pp 1–15
- DIN EN ISO 179-1 (2010) *Plastics-determination of charpy impact properties: part 1: non-instrumented impact test (ISO 179-1:2010)*
- DIN EN ISO 75-1 (2013a) *Plastics-determination of temperature of deflection under load: part 1: general test method (ISO 75-1:2013)*
- DIN EN ISO 75-2 (2013b) *Plastics-determination of temperature of deflection under load: part 2: plastics and ebonite (ISO 75-2:2013)*
- Ecker JV, Kracalik M, Hild S, Haider A (2017) 3D-material extrusion-printing with biopolymers: a review. *Chem Mater Eng* 5(4):83–96. <https://doi.org/10.13189/cme.2017.050402>
- English BW, Falk RH (1995) *Factors that affect the application of woodfiber-plastic composites*. Forest Product Society, Madison, pp 189–194
- Faruk O, Bledzki AK, Fink H-P, Sain M (2012) Biocomposites reinforced with natural fibers: 2000–2010. *Prog Polym Sci* 37(11):1552–1596. <https://doi.org/10.1016/j.progpolymsci.2012.04.003>
- Gebhardt A (2012) *Understanding additive manufacturing: rapid prototyping-rapid tooling-rapid manufacturing*. Carl Hanser Verlag GmbH & Co. KG, Munich
- Geethamma VG, Thomas Mathew K, Lakshminarayanan R, Thomas S (1998) Composite of short coir fibres and natural rubber: effect of chemical modification, loading and orientation of fibre. *Polymer* 39(6–7):1483–1491. [https://doi.org/10.1016/S0032-3861\(97\)00422-9](https://doi.org/10.1016/S0032-3861(97)00422-9)
- Gkartzou E, Koumoulos EP, Charitidis CA (2017) Production and 3D printing processing of bio-based thermoplastic filament. *Manuf Rev* 4:1. <https://doi.org/10.1051/mfreview/2016020>
- Hague R, Campbell I, Dickens P, Reeves P (eds) (2001) *Integration of solid freeform fabrication in design*. In: *Solid freeform fabrication symposium proceedings*, Mechanical Engineering Department, University of Texas at Austin, pp 619–627
- Holbery J, Houston D (2006) Natural-fiber-reinforced polymer composites in automotive applications. *JOM* 58(11):80–86
- Joshi SV, Drzal LT, Mohanty AK, Arora S (2004) Are natural fiber composites environmentally superior to glass fiber reinforced composites? *Compos A Appl Sci Manuf* 35(3):371–376
- Kalia S, Avérous L, Njuguna J, Dufresne A, Cherian BM (2011) Natural fibers, bio- and nanocomposites. *Int J Polym Sci* 2011:2. <https://doi.org/10.1155/2011/735932>
- Kariz M, Sernek M, Obućina M, Kuzman MK (2018) Effect of wood content in FDM filament on properties of 3D printed parts. *Mater Today Commun* 14:135–140. <https://doi.org/10.1016/j.matcom.2017.12.016>
- Le Duigou A, Castro M, Bevan R, Martin N (2016) 3D printing of wood fibre biocomposites: from mechanical to actuation functionality. *Mater Des* 96:106–114. <https://doi.org/10.1016/j.matdes.2016.02.018>
- Lux J, Delisée C, Thibault X (2011) 3D characterization of wood based fibrous materials: an application. *Image Anal Stereol* 25(1):25–35

- Mansour S, Hague R (2003) Impact of rapid manufacturing on design for manufacture for injection moulding. *Proc Inst Mech Eng Part B J Eng Manuf* 217(4):453–461
- Mohanty AK, Misra M, Drzal LT (2002) Sustainable bio-composites from renewable resources: opportunities and challenges in the green materials world. *J Polym Environ* 10(1–2):19–26
- Mohanty AK, Misra M, Drzal LT (2005) Natural fibers, biopolymers, and biocomposites. CRC Press Taylor & Francis Group, Boca Raton. ISBN 978-0-8493-1741-5
- Murphy CA, Collins MN (2018) Microcrystalline cellulose reinforced polylactic acid biocomposite filaments for 3D printing. *Polym Compos* 39(4):1311–1320. <https://doi.org/10.1002/pc.24069>
- ÖNORM EN ISO 527-4 (1997) Plastics-determination of tensile properties: part 4: test conditions for isotropic and orthotropic fibre-reinforced plastic composites (ISO 527-4:1997)
- ÖNORM EN ISO 604 (2003) Plastics-determination of compressive properties (ISO 604:2002)
- Oswald TA (ed) (1999) Fundamental principles of polymer composites: processing and design. In: *Proceeding of 5th International Conference on Wood Fiber-Plastic Composites*, Madison, Wisconsin, USA
- Pandey K (2015) Natural fibre composites for 3D printing. Degree Thesis. Arcada University of Applied Sciences, Helsinki, Finland
- Peltola H, Pääkkönen E, Jetsu P, Heinemann S (2014) Wood based PLA and PP composites: effect of fibre type and matrix polymer on fibre morphology, dispersion and composite properties. *Compos A Appl Sci Manuf* 61:13–22
- Stark NM, Rowlands RE (2003) Effects of wood fiber characteristics on mechanical properties of wood/polypropylene composites. *Wood Fiber Sci* 35(2):167–174
- Summerscales J, Dissanayake N, Virk A, Hall W (2010) A review of bast fibres and their composites. Part 2: composites. *Compos Part A Appl Sci Manuf* 41(10):1336–1344
- Takatani M, Ikeda K, Sakamoto K, Okamoto T (2008) Cellulose esters as compatibilizers in wood/poly (lactic acid) composite. *J Wood Sci* 54(1):54–61
- Tao Y, Wang H, Li Z, Li P, Shi SQ (2017) Development and application of wood flour-filled polylactic acid composite filament for 3D printing. *Materials* 10(4):339. <https://doi.org/10.3390/ma10040339>
- Wang X, Jiang M, Zhou Z, Gou J, Hui D (2017) 3D printing of polymer matrix composites: a review and prospective. *Compos B Eng* 110:442–458. <https://doi.org/10.1016/j.compositesb.2016.11.034>
- Williams GI, Wool RP (2000) Composites from natural fibers and soy oil resins. *Appl Compos Mater* 7(5–6):421–432
- Wimmer R, Steyrer B, Woess J, Koddenberg T, Mundigler N (2015) 3D printing and wood. *Pro Ligno* 11(4):144–149
- Wollerdorfer M, Bader H (1998) Influence of natural fibres on the mechanical properties of biodegradable polymers. *Ind Crops Prod* 8(2):105–112

Publisher's Note Springer Nature remains neutral with regard to jurisdictional claims in published maps and institutional affiliations.